Bright Sub-Poissonian Light through Intrinsic Feedback and External Control

V. S. C. Canela* and H. J. Carmichael†
The Dodd-Walls Centre for Photonic and Quantum Technologies, Department of Physics, University of Auckland, Private Bag 92019, Auckland 1142, New Zealand

(Received 11 August 2019; accepted 22 January 2020; published 14 February 2020)

Balancing nonlinear gain and loss automatically generates sub-Poissonian light, through negative feedback, when the gain is significantly reduced (increased) by the addition (subtraction) of a single photon. We show that micromaser trapping states can provide the necessary feedback in the presence of photon loss and, with the addition of external parametric control, realize a photon number on the order of 100 and a Mandel Q parameter of -0.998, i.e., number squeezing of 27 dB.

DOI: 10.1103/PhysRevLett.124.063604

Sub-Poissonian light has attracted interest in quantum optics since the early 1980s, when its study was first taken up by Short and Mandel following prior observations of photon antibunching in resonance fluorescence [1]. Early measured departures from Poissonian counts [1,2] were small, however, due to photon loss; and while closed loop feedback produced a larger effect [3], the in-loop light is inaccessible and submits to a semiclassical description [4]. Further advances in the 1980s relied on high-impedance suppression of pump fluctuations in semiconductor lasers [5] and light-emitting diodes [6] (see Ref. [7] for a review).

Following these modest beginnings, recent interest may be classified in three distinct categories: (i) development of single-photon sources [8–11], driven by applications, e.g., in linear optical quantum computing and quantum communications; (ii) generation of energy eigenstates of a photon number greater than one, with the experimental observation of states of up to fifteen photons [12–22] and theoretical proposals for arbitrary Fock-state generation [23–28]; and (iii) further work on sub-Poissonian lasers that exploits novel gain characteristics made available by cavity and circuit QED [29–31]. In this Letter, we advance the physics objectives in categories (ii) and (iii). We show that intrinsic feedback, from gain nonlinearity, reduces photon number fluctuations in a conventional laser, but is far too weak to compete with the standard quantum limit. When the gain function is sensitive to the addition or subtraction of one photon, though, the principle is a powerful mechanism for number squeezing; it is especially so in the vicinity of gain function zeros [30–32]. As proof of principle, we show how intrinsic feedback at a stable operating point below a micromaser trapping state can generate a near-Fock state of 126 photons.

Although fundamentally a quantum source of light, the laser operates in a simplest description on the principle of nonlinear gain balancing photon loss. On the gain side, Einstein A and B theory [33] is all that is required to write the balance equation, where for gain provided by N atoms and with n photons in the field [34],

$$T_s^{-1} N n \left(1 - \frac{n}{n_{\rm sat}}\right) = 2\kappa n, \tag{1}$$

where $T_s^{-1} = 4g^2/\gamma_h$ is the stimulated emission rate per photon, 2κ is the photon decay rate, and $n_{\rm sat} = \gamma_\uparrow \gamma_h / 8g^2$ is the saturation photon number; g is the dipole coupling constant, γ_h the homogeneous width, $\gamma_\uparrow$ an excited state injection rate, and the gain-loss ratio in the linear regime defines the pump parameter

$$\wp = N/2\kappa T_s = 2Ng^2/\gamma_h \kappa. \tag{2}$$

Remarkably, the celebrated coherence seems to come for free, a direct consequence of the balance between gain due to stimulated emission and photon loss. It is important in this regard that $n_{\rm sat}$ is large, since it scales the photon number, $n = n_{\rm sat}(\wp - 1)/\wp$, above threshold; it follows that the number uncertainty of a coherent state is only a small perturbation on the balance equation: $n \to n + \delta n$, $\delta n \sim \pm\sqrt{n}$, yields the linearized gain-loss deficit

$$\frac{G(\delta n) - L(\delta n)}{G(0)} = -\frac{1}{\wp}\frac{\delta n}{n_{\rm sat}} \sim \mp\, n_{\rm sat}^{-1/2}. \tag{3}$$

While the negative feedback will work to stabilize n, it is far too weak to reduce fluctuations below the standard quantum limit.

The one-atom micromaser presents a rather different scenario [35,36]. With nonlinear gain provided by a Rabi oscillation of fixed duration T_i, Eq. (1) is replaced by

$$T_i^{-1} N \sin^2\left(g T_i \sqrt{n+1}\right) = 2\kappa n, \tag{4}$$

where, on the gain side, we multiply a flux $T_i^{-1}N$ by the probability that an initially excited atom adds a photon to the field, $n \to n+1$, at T_i. Now the linearized gain-loss deficit is

$$\frac{G(\delta n) - L(\delta n)}{G(0)} = -\frac{\delta n}{S(n)}, \tag{5}$$

where

$$S(n) = \left[\frac{1}{n} - \frac{gT_i}{\sqrt{n+1}}\cot(gT_i\sqrt{n+1})\right]^{-1}. \tag{6}$$

As shown in Fig. 1, stable (S) and unstable (U) operating points lie on curves that pass through zeros of the gain function, i.e., the trapping states [32]

$$n_{\text{trap}}^{(k)} = (k\pi/gT_i)^2 - 1, \quad k = 1, 2, \ldots, \tag{7}$$

where close to the zeros $S(n)$ is small; thus, the operating point at $n = 67$ gives $S(n) = 2.2$ and a gain-loss deficit of nearly $\mp 50\%$ for a change δn of just one photon. In this Letter, we show how this strong negative feedback can be used to generate bright sub-Poissonian light.

We first reproduce and extend the results of Chough and Carmichael [37] demonstrating sub-Poissonian light generation in a quantum trajectory simulation of a free-running micromaser; we thus demonstrate that negative feedback, based on Eq. (6) and Fig. 1, leads automatically to a sub-Poissonian steady state; we also expose various limitations of the free-running approach. The remainder of the Letter discusses the mitigation of these limitations: in a sequence of five steps, we engage external parametric control to progressively improve the results. We quantify this progression by the Mandel Q parameter, $Q = F - 1$, where F is the Fano factor, the ratio of photon number variance to photon number mean: $-10\log F$ is the level of squeezing below the standard quantum limit expressed in decibels.

Pumping of the one-atom micromaser is provided by a stream of qubits, prepared in the excited state, each brought into interaction with a mode of the radiation field

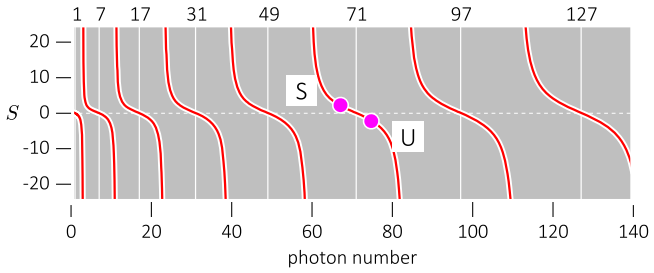

FIG. 1. The function $S(n)$ [Eq. (6)] is plotted for $gT_i = \pi/\sqrt{2}$. Vertical lines locate trapping states (photon numbers above), where $S(n)$ changes sign. Operating points S (U) from Fig. 2 are marked at $n = 67$ (76), $S = 2.2$ (-2.2).

(damped cavity) for an interaction time T_i—a qubit either leaves behind a photon at T_i or it does not. With an average number of simultaneously interacting qubits N and pump rate $T_i^{-1}N$, the gain function of Eq. (4) holds so long as $N \ll 1$. Following [37], we model this scheme for a random qubit stream without the restriction $N \ll 1$; stochastic qubit pumping and photon loss are captured by a three-part quantum trajectory algorithm: (i) Evolution of the unnormalized ket $|\chi(t)\rangle$ under the non-Hermitian Hamiltonian

$$H(t) = \hbar g \sum_{j=1}^{m(t)} (a^\dagger \sigma_-^{(j)} + a\sigma_+^{(j)}) - i\hbar\kappa a^\dagger a, \tag{8}$$

where $m(t)$ is Poisson distributed with mean N, and $\{j\}$ is an ordered labeling of qubits, eigenkets $|\pm\rangle^{(j)}$, brought into interaction at times $\{t_j\}$, $t > t_{m(t)} > t_{m(t)-1} \cdots > t_1 > t - T_i$. (ii) Jumps when a qubit is brought into interaction, at time $t_k \in \{t_j\}$,

$$\begin{aligned} m(t_k) &\to m(t_k) + 1, \\ |\chi(t_k)\rangle &\to |\chi(t_k)\rangle|+\rangle^{(m(t_k)+1)}, \end{aligned} \tag{9}$$

and at time $t_k' = t_k + T_i$, when it is removed,

$$\begin{aligned} m(t_k') &\to m(t_k') - 1, \\ j &\to j - 1, \qquad j = 2, \ldots, m(t_k'), \\ |\chi(t_k')\rangle &\to {}^{(1)}\langle \pm|\chi(t_k')\rangle, \end{aligned} \tag{10}$$

where $|\pm\rangle^{(1)} = |+\rangle^{(1)}$ or $|-\rangle^{(1)}$, as determined by random selection from the probability that the discarded qubit is excited. (iii) Jumps at rate $2\kappa\langle(a^\dagger a)(t)\rangle$ due to photon loss:

$$|\chi(t)\rangle \to a|\chi(t)\rangle. \tag{11}$$

Figures 2(a) and 2(b) present results obtained by time-averaging quantum trajectory simulations of the free-running micromaser. The first trapping state is fixed at $n_{\text{trap}}^{(1)} = 1$ [Eq. (7)] and two values of photon loss are compared: with $2\kappa T_i$ set at 0.001 (0.01), N ranges from 0 to 0.4 (4.0) as the pump parameter, $\wp = N/2\kappa T_i$, varies from 0 to 400. While the lower loss is compatible with the one-qubit gain assumed by Eq. (4), the plots for higher loss encounter multiqubit gain effects with increasing $\wp$: the photon number is raised and becomes less sensitive to trapping states—the oscillations in frame (a) decrease—while oscillations of the Mandel Q parameter are damped [frame (b)]. Note, however, that multiqubit gain cannot be overlooked even for the lower loss, as passing through the trapping states relies on it—the one-qubit gain goes to zero at $n = n_{\text{trap}}^{(k)} = 1, 7, \ldots$.

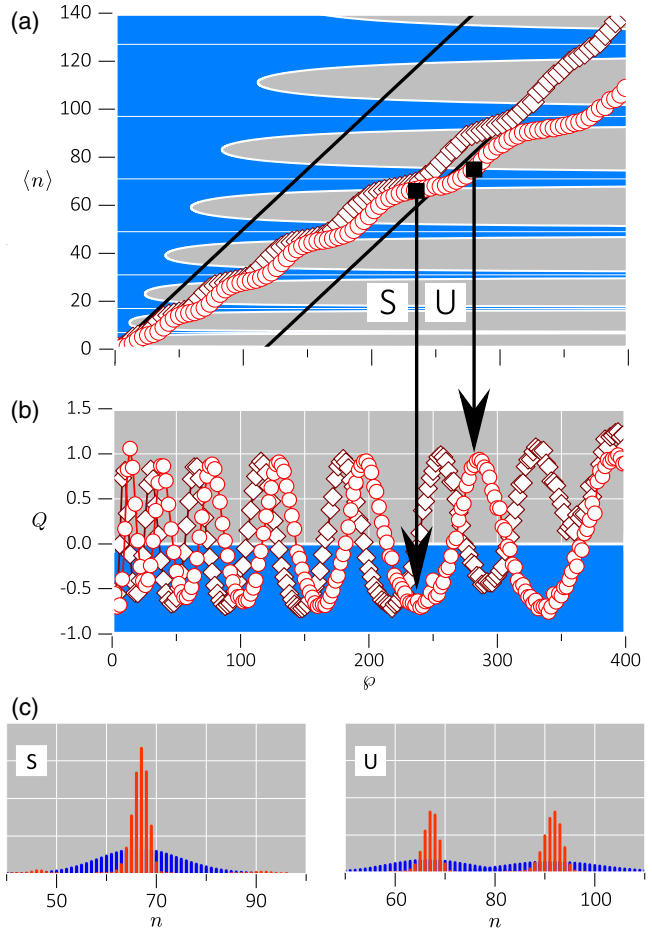

FIG. 2. Quantum trajectory simulation of the free-running micromaser: (a),(b) $\langle n \rangle$ and Mandel Q as a function of pump parameter $\wp$ for $gT_i = \pi/\sqrt{2}$ and $2\kappa T_i = 0.001$ (red circles) and 0.01 (brown diamonds); (c) photon number distributions at stable (S) and unstable (U) operating points compared with Poisson distributions of the same mean. Solutions to Eq. (4) bound shaded regions in (a) and horizontal lines indicate trapping states; the lines $\langle n \rangle = \wp/2$ and $\langle n \rangle = (\wp - 116)/2$ are also shown.

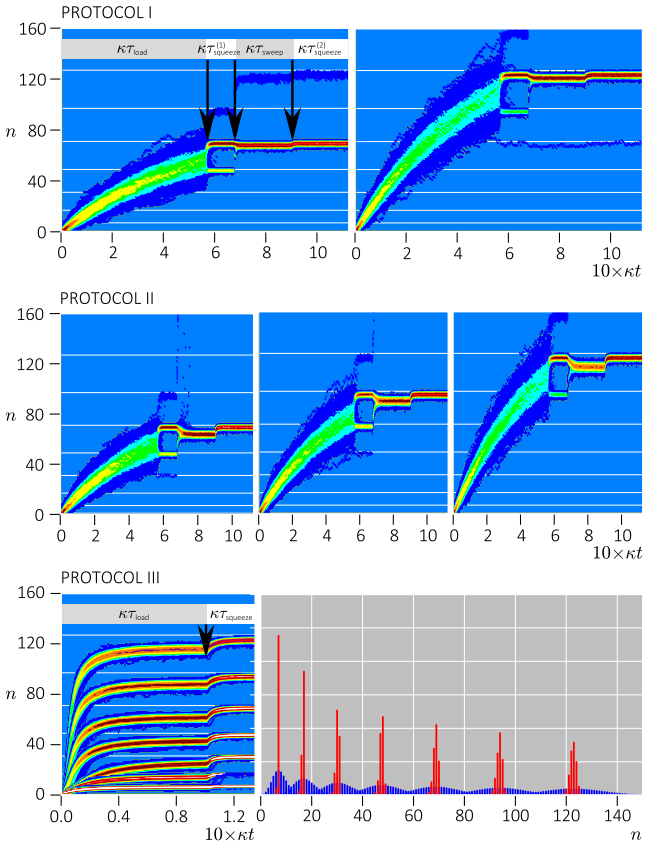

FIG. 3. Preparation of bright sub-Poissonian light by intrinsic feedback and controlled single-photon pumping. Plots follow 1000 quantum trajectories, with trapping states for $gT_i = \pi/\sqrt{2}$ shown as horizontal lines. Protocol I targets the sixth and eighth trapping states, realizing $\langle n \rangle = 69$ and 123, and a local Q of -0.98. Protocol II targets the sixth, seventh, and eighth trapping states, and realizes $\langle n \rangle = 69$, 94, 123; $Q = -0.98$. Protocol III targets the second to eighth tapping states to realize $\langle n \rangle = 7$, 17, 30, 47, 69, 94, 123 and Q ranging from -0.95 (low n) to -0.98 (high n); realized photon number distributions are compared with Poisson distributions of the same mean. All results for $g/2\kappa = (\pi/\sqrt{2}) \times 10^3$.

Our interest lies with the oscillations of the Mandel Q parameter in frame (b), which illustrate the principle, as suggested by Eq. (5) and Fig. 1, that negative feedback will automatically generate bright sub-Poissonian light below the trapping states in the free-running micromaser. Frame (c) shows the sub-Poissonian distribution for the operating point S (stable) on Fig. 1, where a Mandel Q of -0.7 is reached. Even when Q reaches a maximum at the operating point U (unstable), the photon number is *locally* squeezed [frame (d)]; the degraded global Q is the result of switching between metastable states adjacent to the unstable operating point.

We aim now to exploit the demonstrated principle and ultimately lower the Mandel Q from -0.7 to -0.998. Two negative effects of the free-running protocol must initially be overcome: first, the loading of high photon numbers relies on fluctuations of the random pump stream to pass through the trapping states—the process is exceedingly slow and must be speeded up; second, though infrequent, switching from a stable operating point to adjacent states does occur, as evidenced by barely visible peaks at $n = 46$ and 92 in Fig. 2, frame (c). These issues are addressed in the series of three control protocols illustrated in Fig. 3: Protocol III realizes a Q of -0.98 with efficient loading and loss from the targeted trapping state of less than 0.1%. Further control then tightens the squeeze in Fig. 4, where we achieve the ultimate Q of -0.998 with loss to adjacent states reduced to the order of 0.01%.

Protocol I.—Slow loading is overcome by pumping with a stream of qubits assigned random interaction times, i.e., with the nonlinear gain in Eq. (4) replaced by $\langle T_i \rangle^{-1} N/2$, where $\langle T_i \rangle$ is the average time; the mean photon number then grows as

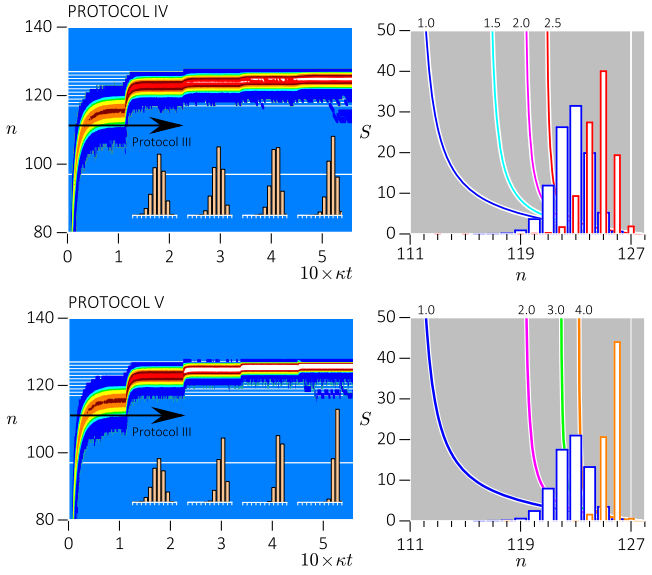

FIG. 4. Progressive squeezing at the eighth trapping state for $gT_i = \pi/\sqrt{2}$. Protocol IV (V) takes steps $1.0T_i$ $(1.0g)$, $1.5T_i$ $(2.0g)$, $2.0T_i$ $(3.0g)$, $2.5T_i$ $(4.0g)$. (Left) Plots follow 10 000 quantum trajectories; the number distribution is progressively squeezed (inset). (Right) Stepped sequence of linearized gain-loss functions $S(n)$ with initial (broad blue) and final (narrow red and orange) photon number distributions superposed and compared. Protocol IV (V) realizes $\langle n\rangle = 124.7$ (125.7) and $Q = -0.991$ (-0.998). All results for $g/2\kappa = (\pi/\sqrt{2}) \times 10^3$.

$$\langle n(t)\rangle = N(4\kappa\langle T_i\rangle)^{-1}(1 - e^{-2\kappa t}), \tag{12}$$

and $\langle T_i\rangle$ may be set to target the negative feedback below a particular trapping state. Random loading takes place during the interval $\kappa\tau_{\rm load}$ in the top frame of Fig. 3, where the target is the sixth (left) and eighth (right) trapping state. Squeezing is incapacitated during random loading, though, so we are left with a Poisson spread in the photon number. The squeezing is now turned on by reverting to fixed T_i and a regular pumping stream for the interval $\kappa\tau^{(1)}_{\rm squeeze}$ in the upper panel of Fig. 3; the photon number is squeezed against the targeted trapping state and the one below with loss on the order of 2%. Finally, we sweep up the population from the state below the targeted trapping state: this is achieved with $T_i \to T_i/2$ (interval $\kappa\tau_{\rm sweep}$), which preserves even trapping states as stable states but destabilizes all odd trapping states; reverting, $T_i/2 \to T_i$, then squeezes against the targeted trapping state again (interval $\kappa\tau^{(2)}_{\rm squeeze}$) and realizes a Mandel Q of -0.98.

Protocol II.—The sweep strategy of Protocol I is limited to the targeting of only even trapping states. We remove this limitation by changing strategy during the interval $\kappa\tau_{\rm sweep}$: instead of $T_i \to T_i/2$, we let $T_i \to T_i^{\rm sweep}$, with $(k_{\rm target} - 1)^{-1} < T_i/T_i^{\rm sweep} < k_{\rm target}^{-1}$, which, according to Eq. (7), places the first new trapping state just below the old targeted state. As illustrated in the middle frame of Fig. 3, this sweeps up everything from below the targeted state and works for both even and odd targets. After reverting—$T_i^{\rm sweep} \to T_i$ in interval $\kappa\tau^{(2)}_{\rm squeeze}$—the same Mandel Q is obtained with similar loss, on the order of 2%.

Protocol III.—The origin of the loss in Protocols I and II is the random interaction time during the loading phase. We now eliminate that loss with a sweep directly out of the vacuum state, following the successful sweep strategy employed in Protocol II. The new two-stage protocol is illustrated in the bottom frame of Fig. 3: during an initial interval $\kappa\tau_{\rm load}$, we set the first trapping state between the targeted state and the one below, i.e., choose $T_i^{\rm load}$ with $(k_{\rm target} - 1)^{-1} < T_i/T_i^{\rm load} < k_{\rm target}^{-1}$; this loads the photons ten times faster while at the same time executing a moderate squeeze; we then revert, $T_i^{\rm load} \to T_i$, during the interval $\kappa\tau_{\rm squeeze}$ to tighten the squeeze. Of the seven targeted trapping states, only $n^{(2)}_{\rm trap}$ suffers any loss at all, to the close adjacent trapping state $n^{(3)}_{\rm trap}$, and the Mandel Q of -0.98 is retained.

Protocols IV and V.—Once a stable operating point is reached, e.g., S in Fig. 1, negative feedback squeezes the photon number between the $S(n)$ asymptote below that operating point and the targeted trapping state above—$n \approx 59$ and $n = 71$ in Fig. 1; the level of squeezing is set by the slope of the linearized gain-loss deficit at the operating point [Eq. (5)]. We now extend Protocol III by increasing the slope. We do so in a three-step sequence, as shown in Fig. 4, in order to preserve photon number confinement. Since $S(n)$ depends on the parameter gT_i [Eq. (6)], we may change either the interaction time T_i (Protocol IV) or the coupling strength g (Protocol V). The Mandel Q of -0.998 is reached in the latter scheme, since it avoids the counteracting effects of larger κT_i.

In summary, progressing from the free-running micromaser through Protocols I–III and on to Protocols IV and V, the Mandel Q is first improved from -0.7 to -0.98 and then from -0.98 to -0.991 and -0.998. Efficient loading of a high photon number is introduced and loss from the targeted trapping state is largely eliminated, with just one of 10 000 trajectories lost in Fig. 4. Although a dipole coupling strength of $g/2\kappa = (\pi/\sqrt{2}) \times 10^3$ is large, it is well within the scope of recent Rydberg atom systems, where photon lifetimes of 65 ms with $g = 2\pi \times 23.5$ kHz [38,39] and 0.2–0.3 s with $g = 2\pi \times 6.5$ kHz [12,13] are realized. Significantly larger coupling strengths of tens to hundreds of megahertz are achieved in circuit QED, and while larger photon loss can offset that increase, single-photon lifetimes for 3D cavities approaching 10 μs [40], and even a remarkable 10 ms [41], have been reported.

Even Protocols I-III and Protocol IV realize significant squeezing, where the Qs of -0.98 and -0.991 correspond, respectively, to squeezing of 17 and 20 dB; Protocol V then stands apart with a Q of -0.998 and squeezing of 27 dB. Note that only Protocol V requires control of the coupling

strength, as the manipulations of Protocols I–IV are carried out by changing the interaction time. While real-time control presents an experimental challenge in either case, the interaction time is probably the easier of the two parameters to change: qubits might be switched in and out of cavity resonance in a circuit QED setting, or different velocity selected streams of atoms might be used in a Rydberg atom system; changing the coupling strength would likely require switching between distinct qubits for each desired setting, or, if moving atoms are used, different transits through a structured cavity mode.

Although 27 dB squeezing (Protocol V) presents a large experimental challenge and is likely only a distant goal, our proposal builds upon a simple and robust mechanism, intrinsic feedback, which is worthy of further attention. The generation of sub-Poissonian light in this approach potentially has broad application, even to optical systems where coupling strengths are less strong, albeit with less extreme results. We also note that while, as described, Protocols I–V prepare the state of a mode inside a cavity, subsequent free decay to either waveguide or free-space modes would output a pulse; alternatively, extending the time axis of Figs. 3 and 4 provides a steady stream of output photons after the manner of Refs. [29] and [31].

We are grateful to Young-Tak Chough for discussions and access to his initial quantum trajectory code. V. S. C. C. acknowledges the support of the New Zealand Tertiary Education Committee through the Dodd-Walls Centre for Photonic and Quantum Technologies. We thank the Center for eResearch, University of Auckland, for their support providing access to the NeSI Pan Cluster where many of the quantum trajectory simulations were carried out.

*vsan819@aucklanduni.ac.nz
†h.carmichael@auckland.ac.nz

[1] R. Short and L. Mandel, Observation of Sub-Poissonian Photon Statistics, Phys. Rev. Lett. **51**, 384 (1983).
[2] M. C. Teich and B. E. A. Saleh, Observation of sub-Poissonian Franck-Hertz light at 253.7 nm, J. Opt. Soc. Am. B **2**, 275 (1985).
[3] S. Machida and Y. Yamamoto, Observation of sub-Poissonian photoelectron statistics in a negative feedback semiconductor laser, Opt. Commun. **57**, 290 (1986).
[4] J. G. Rarity, P. R. Tapster, and E. Jakeman, Observation of sub-Poissonian light in parametric downconversion, Opt. Commun. **62**, 201 (1987).
[5] P. R. Tapster, J. G. Rarity, and J. S. Satchel, Observation of Amplitude Squeezing in a Constant-Current-Driven Semiconductor Laser, Phys. Rev. Lett. **58**, 1000 (1987).
[6] J. G. Rarity, P. R. Tapster, and J. S. Satchell, Generation of sub-Poissonian light by high-efficiency light-emitting diodes, Europhys. Lett. **4**, 293 (1987).
[7] L. Davidovich, Sub-Poissonian processes in quantum optics, Rev. Mod. Phys. **68**, 127 (1996).
[8] M. D. Eisaman, J. Fan, A. Migdall, and S. V. Polyakov, Invited Review Article: Single-photon sources and detectors, Rev. Sci. Instrum. **82**, 071101 (2011).
[9] C. J. Cunnilall, I. P. Degiovanni, S. Kück, I. Müller, and A. G. Sinclair, Metrology of single-photon sources and detectors: a review, Opt. Eng. **53**, 081910 (2014).
[10] N. Somaschi, V. Giesz, L. De Santis, J. C. Loredo, M. P. Almeida, G. Hornecker, S. L. Portalupi, T. Grange, C. Antón, J. Demory, C. Gómez, I. Sagnes, N. D. Lanzillotti-Kimura, A. Lemaítre, A. Auffeves, A. G. White, L. Lanco, and P. Senellart, Near-optimal single-photon sources in the solid state, Nat. Photonics **10**, 340 (2016).
[11] P. Senellart, G. Solomon, and A. White, High-performance semiconductor quantum-dot single-photon sources, Nat. Nanotechnol. **12**, 1026 (2017).
[12] B. T. H. Varcoe, S. Brattke, M. Weidinger, and H. Walther, Preparing pure photon number states of the radiation field, Nature (London) **403**, 743 (2000).
[13] S. Brattke, B. T. H. Varcoe, and H. Walther, Generation of Photon Number States on Demand via Cavity Quantum Electrodynamics, Phys. Rev. Lett. **86**, 3534 (2001).
[14] P. Bertet, S. Osnaghi, P. Milman, A. Auffeves, P. Maioli, M. Brune, J. M. Raimond, and S. Haroche, Generating and Probing a Two-Photon Fock State with a Single Atom in a Cavity, Phys. Rev. Lett. **88**, 143601 (2002).
[15] C. Sánchez Monõz, F. P. Laussy, C. Tejedor, and E. del Valle, Enhanced two-photon emission from a dressed biexciton, New J. Phys. **17**, 123021 (2015).
[16] E. Sánchez-Burillo, L. Martín-Moreno, J. J. García-Ripoll, and D. Zueco, Full two-photon down-conversion of a single photon, Phys. Rev. A **94**, 053814 (2016).
[17] Y. Chang, A. González-Tudela, C. Sánchez Munõz, C. Navarrete-Benlloch, and T. Shi, Deterministic Down--Converter and Continuous Photon-Pair Source within the Bad-Cavity Limit, Phys. Rev. Lett. **117**, 203602 (2016).
[18] E. Waks, E. Diamanti, and Y. Yamamoto, Generation of photon number states, New J. Phys. **8**, 4 (2006).
[19] C. Guerlin, J. Bernu, S. Deléglise, C. Sayrin, S. Gleyses, S. Kuhr, M. Brune, J. M. Raimond, and S. Haroche, Progressive field-state collapse and quantum non--demolition photon counting, Nature (London) **448**, 889 (2007).
[20] M. Hofheinz, E. M. Weig, M. Ansmann, R. C. Bialczak, E. Lucero, M. Neeley, A. D. O'Connell, H. Wang, J. M. Martinis, and A. N. Cleland, Generation of Fock states in a superconducting quantum circuit, Nature (London) **454**, 310 (2008).
[21] H. Wang, M. Hofheinz, M. Ansmann, R. C. Bialczak, E. Lucero, M. Neeley, A. D. O'Connell, D. Sank, J. Wenner, A. N. Cleland, and J. M. Martinis, Measurement of the Decay of Fock States in a Superconducting Quantum Circuit, Phys. Rev. Lett. **101**, 240401 (2008).
[22] X. Zhou, I. Dotsenko, B. Peaudecerf, T. Rybarczyk, C. Sayrin, S. Gleyzes, J. M. Raimond, M. Brune, and S. Haroche, Field Locked to a Fock State by Quantum Feedback with Single Photon Correlations, Phys. Rev. Lett. **108**, 243602 (2012).
[23] K. R. Brown, K. M. Dani, D. M. Stamper-Kurn, and K. B. Whaley, Deterministic optical Fock-state generation, Phys. Rev. A **67**, 043818 (2003).

[24] J. M. Geremia, Deterministic and Nondestructively Verifiable Preparation of Photon Number States, Phys. Rev. Lett. **97**, 073601 (2006).
[25] C. Sánchez Moñoz, E. del Valle, A. González Tudela, K. Müller, S. Lichtmannecker, M. Kaniber, C. Tajedor, J. J. Finley, and F. P. Laussy, Emitters of N-photon bundles, Nat. Photonics **8**, 550 (2014).
[26] A. González-Tudela, V. Paulisch, D. E. Chang, H. J. Kimble, and J. I. Cirac, Deterministic Generation of Arbitrary Photonic States Assisted by Dissipation, Phys. Rev. Lett. **115**, 163603 (2015).
[27] A. González-Tudela, V. Paulisch, H. J. Kimble, and J. I. Cirac, Efficient Multiphoton Generation in Waveguide Quantum Electrodynamics, Phys. Rev. Lett. **118**, 213601 (2017).
[28] C. Sánchez Moñoz, F. P. Laussy, E. del Valle, C. Tejedor, and A. González-Tudela, Filtering multiphoton emission from state-of-the-art cavity quantum electrodynamics, Optica **5**, 14 (2018).
[29] W. Choi, J.-H. Lee, K. An, C. Fang-Yen, R. R. Dasari, and M. S. Feld, Observation of Sub-Poissonian Photon Statistics in the Cavity-QED Microlaser, Phys. Rev. Lett. **96**, 093603 (2006).
[30] M. Koppenhöfer and M. Marthaler, Creation of a squeezed photon distribution using artificial atoms with broken inversion symmetry, Phys. Rev. A **93**, 023831 (2016).
[31] M. Koppenhöfer, J. Leppäkangas, and M. Marthaler, Creating photon-number squeezed strong microwave fields by a Cooper-pair injection laser, Phys. Rev. B **95**, 134515 (2017).
[32] P. Meystre, G. Rempe, and H. Walther, Very-low-temperature behavior of a micromaser, Opt. Lett. **13**, 1078 (1988).
[33] A. Einstein, Strahlungs-emission und -absorption nach der Quantentheorie, Verh. Dtsch. Phys. Ges. **18**, 318 (1916); Zur Quantentheorie der Strahlung, Phys. Z. **18**, 121 (1917).
[34] H. J. Carmichael, *Statistical Methods in Quantum Optics* (Springer, Berlin, 1999), Vol. 1.
[35] D. Meschede, H. Walther, and G. Müller, One-Atom Maser, Phys. Rev. Lett. **54**, 551 (1985).
[36] P. Filipowicz, J. Javanainen, and P. Meystre, Theory of a microscopic maser, Phys. Rev. A **34**, 3077 (1986).
[37] Y.-T. Chough and H. J. Carmichael, Micromaser revisited: Sub-Poissonian fields from Poissonian pumping, J. Phys. Soc. Jpn. **82**, 014401 (2013).
[38] S. Kuhr, S. Gleyzes, C. Guerlin, J. Bernu, U. B. Hoff, S. Deléglise, S. Osnaghi, M. Brune, J. M. Raimond, S. Haroche, E. Jacques, P. Bosland, and B. Visentin, Ultrahigh finesse Fabry-Pérot superconducting resonator, Appl. Phys. Lett. **90**, 164101 (2007).
[39] S. Gleyzes, S. Kuhr, C. Guerlin, J. Bernu, S. Deléglise, U. B. Hoff, M. Brune, J. M. Raimond, and S. Haroche, Quantum jumps of light recording the birth and death of a photon in a cavity, Nature (London) **446**, 297 (2007).
[40] J. R. A. Müller, 3D cavities for circuit quantum electrodynamics, Bachelor's thesis, Technische Universität München, 2014.
[41] M. Reagor, H. Paik, G. Catelani, L. Sun, C. Axline, E. Holland, I. M. Pop, M. A. Masluk, T. Brecht, L. Frunzio, M. H. Devoret, L. Glazman, and R. J. Schoelkopf, Reaching 10 ms single photon lifetimes for superconducting aluminum cavities, Appl. Phys. Lett. **102**, 192604 (2013).